Manuscript version: Published Version
The version presented in WRAP is the published version (Version of Record).

Persistent WRAP URL:
http://wrap.warwick.ac.uk/62800

How to cite:
The repository item page linked to above, will contain details on accessing citation guidance from the publisher.

Copyright and reuse:
The Warwick Research Archive Portal (WRAP) makes this work by researchers of the University of Warwick available open access under the following conditions.

Copyright © and all moral rights to the version of the paper presented here belong to the individual author(s) and/or other copyright owners. To the extent reasonable and practicable the material made available in WRAP has been checked for eligibility before being made available.

Copies of full items can be used for personal research or study, educational, or not-for-profit purposes without prior permission or charge. Provided that the authors, title and full bibliographic details are credited, a hyperlink and/or URL is given for the original metadata page and the content is not changed in any way.

Publisher's statement:
Please refer to the repository item page, publisher's statement section, for further information.

For more information, please contact the WRAP Team at: wrap@warwick.ac.uk

Controlling Magnetic Order and Quantum Disorder in Molecule-Based Magnets

T. Lancaster,[1,*] P. A. Goddard,[2] S. J. Blundell,[3] F. R. Foronda,[3] S. Ghannadzadeh,[3] J. S. Möller,[3] P. J. Baker,[4] F. L. Pratt,[4] C. Baines,[5] L. Huang,[6] J. Wosnitza,[6] R. D. McDonald,[7] K. A. Modic,[7] J. Singleton,[7] C. V. Topping,[7] T. A. W. Beale,[1] F. Xiao,[1] J. A. Schlueter,[8,†] A. M. Barton,[9] R. D. Cabrera,[9] K. E. Carreiro,[9] H. E. Tran,[9] and J. L. Manson[9,‡]

[1]*Durham University, Centre for Materials Physics, South Road, Durham DH1 3LE, United Kingdom*
[2]*Department of Physics, University of Warwick, Coventry CV4 7AL, United Kingdom*
[3]*Department of Physics, Clarendon Laboratory, Oxford University, Parks Road, Oxford OX1 3PU, United Kingdom*
[4]*ISIS Facility, Rutherford Appleton Laboratory, Chilton, Oxfordshire OX11 0QX, United Kingdom*
[5]*Laboratory for Muon-Spin Spectroscopy, Paul Scherrer Institut, CH-5232 Villigen PSI, Switzerland*
[6]*Dresden High Magnetic Field Laboratory, Helmholtz-Zentrum Dresden-Rossendorf, D-01314 Dresden, Germany*
[7]*National High Magnetic Field Laboratory, Los Alamos National Laboratory, MS-E536, Los Alamos, New Mexico 87545, USA*
[8]*Materials Science Division, Argonne National Laboratory, Argonne, Illinois 60439, USA*
[9]*Department of Chemistry and Biochemistry, Eastern Washington University, Cheney, Washington 99004, USA*
(Received 29 November 2013; revised manuscript received 17 March 2014; published 19 May 2014)

We investigate the structural and magnetic properties of two molecule-based magnets synthesized from the same starting components. Their different structural motifs promote contrasting exchange pathways and consequently lead to markedly different magnetic ground states. Through examination of their structural and magnetic properties we show that $[Cu(pyz)(H_2O)(gly)_2](ClO_4)_2$ may be considered a quasi-one-dimensional quantum Heisenberg antiferromagnet whereas the related compound $[Cu(pyz)(gly)](ClO_4)$, which is formed from dimers of antiferromagnetically interacting Cu^{2+} spins, remains disordered down to at least 0.03 K in zero field but shows a field-temperature phase diagram reminiscent of that seen in materials showing a Bose-Einstein condensation of magnons.

A goal of research in magnetism is to gain control of chemical components in order that desirable magnetic behavior may be achieved [1,2]. This relies on a detailed understanding of the relationship between starting materials, structure, and magnetic properties. Here, we present a case based on the manipulation of molecular building blocks, where a synthetic route leads to the realization of two structurally distinct materials based on similar chemical components. The resulting systems possess different low-dimensional motifs that promote one- and zero-dimensional magnetic behavior, respectively. Through magnetometry, heat capacity, electron paramagnetic resonance (EPR), and muon-spin relaxation (μ^+SR) we show that these materials represent realizations of different models of quantum magnetism in reduced dimensions, namely, (i) the quasi one-dimensional $S = 1/2$ quantum Heisenberg antiferromagnet (1DQHAF) [3] and (ii) an assembly of weakly coupled singlet dimers (each one composed of two antiferromagnetically coupled $S = 1/2$ spins) with a quantum disordered ground state that may be driven with an applied magnetic field via a quantum critical point (QCP) into a magnetic phase reminiscent of the Bose-Einstein condensation (BEC) of magnons [4]. The wealth of recent research interest in the BEC problem in magnetic insulators [5] has motivated us to elucidate the phase diagram of the latter system, which has the potential to provide insight into the realization and manipulation of quantum states more generally.

The synthesis of the materials (described in full in the Supplemental Material [6]) involves mixing aqueous solutions of $Cu(ClO_4)_2 \cdot 6H_2O$, glycine [NH_2CH_2COOH, (gly)], and pyrazine [$C_4H_4N_2$, (pyz)]. Purple blocks of $[Cu(pyz)(gly)](ClO_4)$ typically form first upon slow evaporation of the solvent, while continued evaporation leads to the formation of blue rods of $[Cu(pyz)(H_2O)(gly)_2](ClO_4)_2$. Despite the presence of the same molecular components, the infrared spectra of these materials differ markedly between 1300 and 1700 cm^{-1}, allowing their identification and isolation. Varying the relative ratios of chemical reagents does not alter the outcome, and the latter material is always obtained in higher yield.

The structure of $[Cu(pyz)(H_2O)(gly)_2](ClO_4)_2$, which crystallizes in space group $C2/c$, is based on linear chains of $S = 1/2$ Cu^{2+} ions linked with pyz ligands as shown in Fig. 1(a). Glycine groups and H_2O molecules coordinate with the Cu^{2+} ions and these, along with noncoordinating ClO_4^- counterions, act to separate the chains [Fig. 1(b)]. The pyz ligand is known to be an effective mediator of magnetic exchange in materials of this type, and so we would expect the chainlike structure to promote one-dimensional (1D) antiferromagnetic behavior. In contrast, the structure of $[Cu(pyz)(gly)](ClO_4)$ (space group $P2_1/n$) is based on a lattice of alternating Cu^{2+} dimers as shown in Figs. 1(c) and 1(d). The two Cu^{2+} ions in a dimer are coupled by a pyz ligand, and these dimers are tethered with gly bridges that connect the dimers to form corrugated
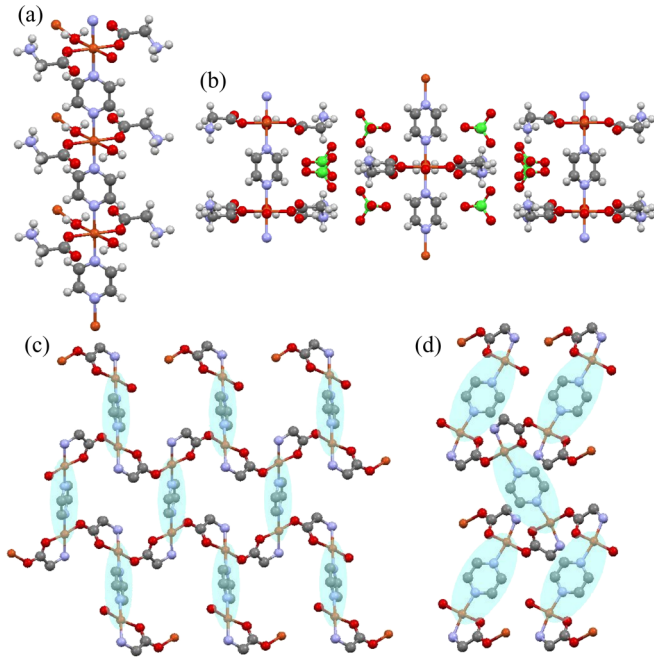
FIG. 1 (color online). (a) Cu-(pyz)-Cu chains on which $[Cu(pyz)(H_2O)(gly)_2](ClO_4)_2$ is based. Water and gly groups that coordinate with the Cu ions are also shown. (b) The material viewed along the c axis showing the packing of the chains with noncoordinating ClO_4 groups. $[Cu(pyz)(gly)](ClO_4)$ viewed along (c) the a axis and (d) the c axis showing pairs of Cu^{2+} ions strongly coupled through pyz ligands to form alternating dimers. (Dimers are shaded, and the ClO_4 ions have been removed for clarity).

sheets, with noncoordinating ClO_4^- ions lying between these sheets. The exchange through gly groups and ClO_4^- ions might be expected to be comparatively weak, suggesting that the physics of this material is due to dimer units weakly coupled with their neighbors.

The magnetic behavior of chainlike $[Cu(pyz)(H_2O)(gly)_2](ClO_4)_2$ was characterized using magnetic susceptibility and magnetization measurements on polycrystalline samples and found to be well described by the predictions of the 1DQHAF model. This model is defined by a Hamiltonian

$$H = J\sum_{\langle i,j\rangle\|}S_i\cdot S_j + J_\perp\sum_{\langle i,j\rangle\perp}S_i\cdot S_j - g\mu_B B\sum_i S_i^z, \quad (1)$$

where J is the strength of the exchange coupling within the magnetic chains, $J_\perp$ is the coupling between chains, and the first and second summations refer to summing over unique pairs of nearest neighbors parallel and perpendicular to the chain, respectively. The magnetic susceptibility [shown in inset in Fig. 2(a)] is well described by the form expected [7] for the model in Eq. (1) with antiferromagnetic (AF) intrachain exchange strength $|J| = 9.4(1)$ K and $g = 2.10(1)$. Magnetization measurements are shown in
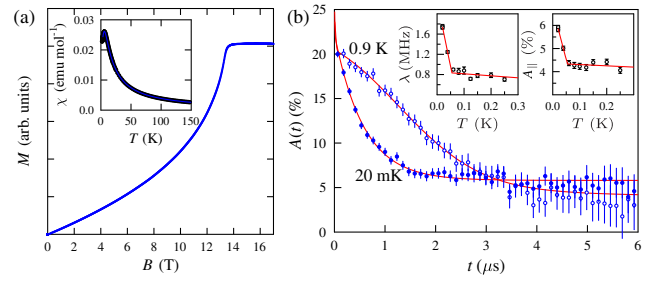

FIG. 2 (color online). (a) Magnetization of chainlike $[Cu(pyz)(H_2O)(gly)_2](ClO_4)_2$ measured at 0.5 K. Inset: magnetic susceptibility measured in an applied field of 100 mT. (b) ZF μ^+SR spectra measured at 0.9 and 0.02 K. Inset: Relaxation rate and nonrelaxing amplitude (right) as a function of temperature showing the onset of the magnetic transition.

Fig. 2(a) and have a concave curvature typical of a quasi-1D system. The saturation field of the magnetization $B_c = 13.3(1)$ T allows us to estimate the exchange since we expect $g\mu_B B_c = 2J + 4J_\perp$. Assuming $J_\perp/J \ll 1$ suggests $J = 9.4(1)$ K , in agreement with the results above. We note that this value is quite typical of exchange through Cu-pyz-Cu bonds [2,8].

In order to assess how well $[Cu(pyz)(H_2O)(gly)_2](ClO_4)_2$ approximates a 1DQHAF, we use the ratio of the magnetic ordering temperature T_N to J. This should be zero for an ideal 1D magnet and close to unity for an isotropic system. Many thermodynamic probes cannot resolve the ordering transition in 1D systems owing to strong thermal and quantum fluctuations, which lower the magnitude of T_N, resulting in correlations with sizeable correlation length building up in the chains just above the ordering temperature and also reducing the magnitude of the magnetic moment [9]. We have shown previously [2,10] that muons are often sensitive to long-range magnetic order (LRO) that can be very difficult to detect with thermodynamic probes in quasi-1D systems.

Example zero-field (ZF) μ^+SR spectra are shown in Fig. 2(b). Although oscillations, characteristic of a quasi-static local magnetic field at the muon stopping site, are not observed at any temperature, we do see a sudden change in behavior at low temperature that is evidence for magnetic order. Data were well described across the measured temperature range by a function

$$A(t) = A_1 e^{-\sigma_1^2 t^2} + A_2 e^{-\sigma_2^2 t^2} + A_3 e^{-\lambda t} + A_\|, \quad (2)$$

where the first term captures the rapid relaxation observed at early times and the term with amplitude A_2 captures the weak relaxation due to disordered nuclear moments. As the temperature is lowered, we observe a sharp increase in both the relaxation rate λ (reflecting the behavior of electronic moments) and the baseline amplitude $A_\|$ around 40 mK. This behavior, which has been observed previously in chainlike materials of this type [2], is strongly indicative of

magnetic order. The change in shape in the spectrum results from the muon being insensitive to the rapid fluctuations of the electronic moments (on the muon time scale) for $T > T_N$ but being relaxed by these upon their static ordering. At the low temperatures involved, we are unable to see the response saturate at the lowest temperatures and so, strictly speaking, we should assign the onset of the change in behavior as an upper bound on T_N. From this, we estimate $T_N \leq 0.04(1)$ K for $[Cu(pyz)(H_2O)(gly)_2](ClO_4)_2$.

Quantum Monte Carlo simulations provide a means of estimating the effective interchain coupling $J_\perp$ in a quasi-1D antiferromagnet via the expression [11]

$$|J_\perp| = \frac{T_N}{4c\sqrt{\ln(\frac{aJ}{T_N}) + \frac{1}{2}\ln \ln(\frac{aJ}{T_N})}}, \qquad (3)$$

where $c = 0.233$ and $a = 2.6$ for $S = 1/2$ spins. Using our values of T_N and J, we obtain an estimate $|J_\perp/J| \lesssim 2 \times 10^{-3}$, which provides a measure of the degree to which $[Cu(pyz)(H_2O)(gly)_2](ClO_4)_2$ realizes the 1DQHAF (for which $|J_\perp/J| = 0$). It, therefore, provides a more isolated realization of the 1DQHAF than $Cu(pyz)(NO_3)_2$ ($|J_\perp/J| = 4.4 \times 10^{-3}$) [10] but is probably less well isolated than Sr_2CuO_3 ($|J_\perp/J| = 7 \times 10^{-4}$) [12] and $DEOCC\text{-}TCNQF_4$ ($|J_\perp/J| < 6 \times 10^{-5}$) [13].

We now turn to the magnetic properties of $[Cu(pyz)(gly)](ClO_4)$. The results of magnetic susceptibility measurements on single crystal samples are shown in Fig. 3(a) with a magnetic field applied along the long axis of a crystallite. These data are well described by the Bleaney-Bowers model [14], which gives the susceptibility of a system of isolated antiferromagnetically coupled dimers and yields an intradimer exchange strength of $|J_0| = 7.5(1)$ K. A slightly better fit may be obtained assuming a mean-field ferromagnetic (FM) interdimer coupling, resulting in an AF intradimer coupling of $|J_0| = 8.1(1)$ K and FM coupling $J \approx 2$ K. We note that such fits are quite sensitive to the details of the model used (we return to the nature of this coupling below). Our ZF μ^+SR measurements show no indication of magnetic order or sizeable relaxation due to fluctuating electronic moments with the spectra [Fig. 3(e)] remaining typical of relaxation due to disordered nuclear magnetism on cooling to 32 mK (see the Supplemental Material [6]).

These results suggest that $[Cu(pyz)(gly)](ClO_4)$ should be described via a Hamiltonian

$$H = J_0\sum_i \mathbf{S}_{1,i} \cdot \mathbf{S}_{2,i} + \sum_{\langle mnij \rangle} J_{mnij}\mathbf{S}_{m,i} \cdot \mathbf{S}_{n,j} - g\mu_B B\sum_{\langle mi \rangle} S^z_{m,i}, \qquad (4)$$

where i, j label dimers and $m, n = 1, 2$ label their magnetic sites [4]. If J_{mnij} are weak compared to the antiferromagnetic intradimer exchange J_0, then this causes the ground
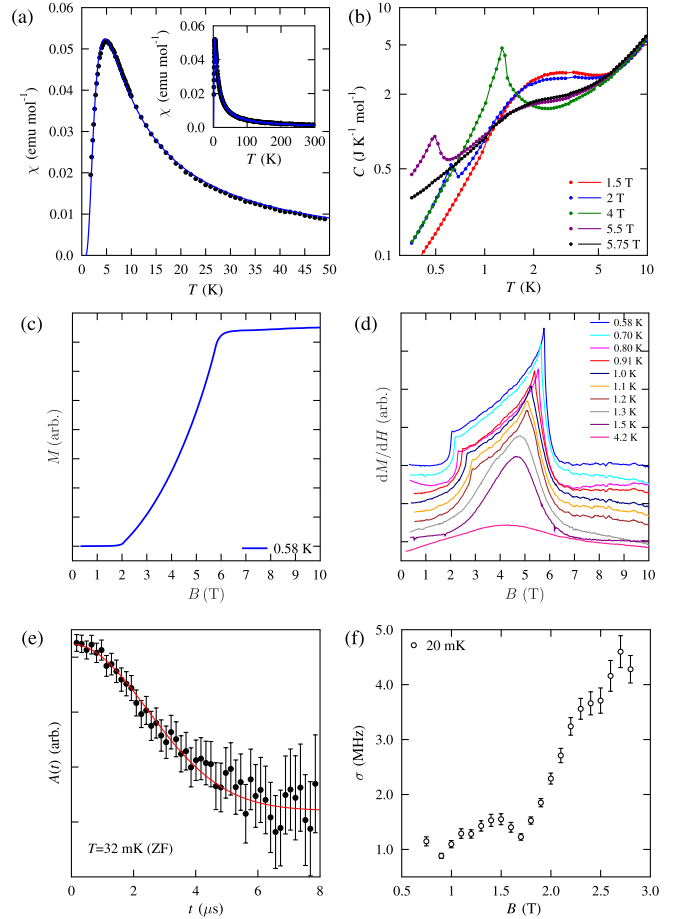

FIG. 3 (color online).   (a) Static magnetic susceptibility data for $[Cu(pyz)(gly)](ClO_4)$ measured in a field of 5 mT. A fit is shown to the Bleaney-Bowers model of noninteracting dimers. (b) Heat capacity showing magnetic transitions in applied magnetic fields. (c) Magnetization at 0.58 K and (d) dynamic susceptibility dM/dH at several temperatures showing sharp features at the phase transitions (data offset for each temperature for clarity). (e) Example ZF μ^+SR spectrum measured at 32 mK showing no signature of long-range magnetic order. (f) Relaxation rate at 20 mK as a function of transverse applied magnetic field showing a transition around 1.7 T.

state to be one of quantum disorder, formed from an array of $S = 0$ spin singlets.

The application of a magnetic field is found to drive this material through a magnetic phase transition. The transition is seen in heat capacity, dynamic magnetic susceptibility, and μ^+SR measurements made on $[Cu(pyz)(gly)](ClO_4)$. As shown in Fig. 3(b), sharp peaks are observed in heat capacity measurements on a single crystal [with the field applied as for the static susceptibility shown in Fig. 3(a)] in the 2–6 T region in scans across the temperature range $0.4 < T < 1.4$ K. Single crystal, dynamic magnetic susceptibility measurements were performed using a radio-frequency based susceptometer [6,15]. The dynamic susceptibility $\chi = dM/dH$ was measured in two different

orientations, with the magnetic field applied close to normal to the (110) or (122) crystallographic planes. The field for the (110) orientation is parallel to the *a-b* plane, which contains the dimers. The phase transitions may be identified from the sharp features in χ, shown in Fig. 3(d). The magnetization at 0.58 K, found from integration of χ, is shown in Fig. 3(c). Transitions are also observed in μ^+SR (for which an unaligned polycrystalline sample was measured) using both a transverse field (TF) geometry (with initial muon spin perpendicular to the applied field) and in a longitudinal field (LF) geometry (initial muon spin parallel to the applied field) (see the Supplemental Material [6]). The form of the transition in the TF geometry [Fig. 3(f)] involves a rapid rise in relaxation and is similar to that observed for field-induced transitions in molecular magnets of this sort [16] and also in the candidate BEC material $Pb_2V_3O_9$ [17]. In the LF data, the phase boundary is identified via a sudden change in the integrated asymmetry and in the relaxation rate (Supplemental Material [6]).

The positions of the phase boundaries determined by the different measurements show some degree of dependence on the crystal orientation, reflecting the effect of *g*-factor anisotropy. Our EPR measurements (Supplemental Material [6]) allow us to determine the *g* factor for fields applied normal to the (110) plane as $g^{(110)} = 2.18$. The phase boundaries are found to coincide if we take $g^{(122)} = 2.15$ for the dynamic susceptibility with the other measured crystal orientation, $g^{\mu SR} = 2.20$ for μ^+SR and $g^{HC} = 2.30$ for heat capacity. (We note that these *g* factors all fall within the range typically found in Cu-based coordination polymers [2,8].) Scaling the field B_c at which the phase change occurs for each measurement by plotting $g\mu_B B_c$, we obtain the phase diagram shown in Fig. 4. which, as shown below, is consistent with that of a system of AF dimers, with weak FM interdimer coupling [18].

The phase diagram results from the fact that at temperatures well below the intradimer separation $|J_0|$, the ground state is a quantum-disordered paramagnet formed from a sea of singlets [4,5,18,19]. The applied field (which we assume is along *z*) closes the singlet-triplet spin gap at a QCP at $g\mu_B B_{c1}$, leading to a state of LRO formed from the transverse spin components $\langle S_x \rangle$ and $\langle S_y \rangle$, which spontaneously break the $O(2)$ symmetry of the spin Hamiltonian. Further application of the field for $B > B_{c1}$ cants the spin components along *z* until we encounter the fully *z*-polarized FM phase beyond another QCP at $g\mu_B B_{c2}$. In the mean-field approximation, the upper phase boundary for FM coupled dimers occurs at the intradimer exchange value $g\mu_B B_{c2} = |J_0|$ which we estimate from the phase boundary to be 9.0(2) K, broadly consistent with, but slightly larger than, the value derived from dc susceptibility, but in agreement with the expected value for AF exchange mediated by a pyz group (such as that in $[Cu(pyz)(H_2O)(gly)_2](ClO_4)_2$ above). The mean-field
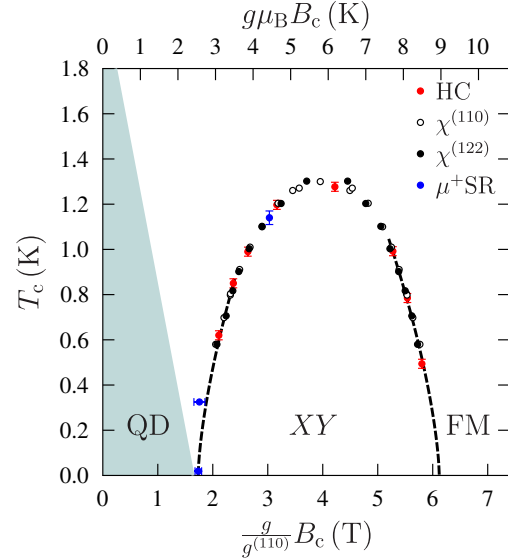

FIG. 4 (color online). The *B-T* phase diagram for $[Cu(pyz)(gly)](ClO_4)$, showing quantum critical points at $g\mu_B B_c = 2.5(1)$ and 9.0(2) K. Dashed line shows the expected behavior of the phase boundaries with exponent $\phi = 2/3$, predicted for the BEC of magnons model.

model also predicts that $g\mu_B B_{c1} = |J_0| - \alpha|J_1|/2$, where α is the number of interacting nearest neighbors linked with a mean-field FM interdimer exchange constant $J_1(= \langle J_{mnij} \rangle)$. We find $g\mu_B B_{c1} = 2.5(1)$ K, and so, assuming $\alpha = 4$, we obtain $|J_1| \approx 3.3(1)$ K. If, instead, an AF interdimer coupling is assumed [18], we would obtain $|J_0| = 4.5$ K, which is not compatible with the dc susceptibility measurement.

Dimer systems such as these are often discussed in the context of the BEC of magnons, which provides a similar description of the physics in terms of a transition from a triplon vacuum at low field to a Bose condensed state that breaks a global $U(1)$ symmetry, isomorphic to the $O(2)$ invariance of the isolated dimer system in magnetic field [4,5,19]. The BEC picture predicts phase boundaries with a $\phi = 2/3$ power law exponent, which is not inconsistent with our data, although the paucity of data points in the critical region prevents this from being rigorously assessed. Although this material may provide a further approximate realization of a magnon BEC, we note that $O(2)[\equiv U(1)]$ symmetry is essential for the realization of the model and we cannot rule out a small Dzyaloshinsky-Moriya (DM) interaction [20] providing a term in the Hamiltonian $\mathbf{D} \cdot (\mathbf{S}_1 \times \mathbf{S}_2)$ that may break the XY symmetry in the *a-b* plane. Although inversion centers exist between neighboring dimer centers with the same orientation shown in Fig. 1(d), the neighbors with different orientations are symmetry related through a glide plane. This implies a nonzero DM interaction with strength $\mathbf{D}$ within the *a-b* plane.

In conclusion, we have shown how a chemical synthesis route leads to two separable phases of matter whose

difference in structure allows them to realize two distinct models of quantum magnetism distinguished by their dimensionality. The first is a good realization of a $S = 1/2$ 1DQHAF, which shows magnetic order at very low temperature. The other is based on magnetic dimers giving rise to a quantum disordered ground state and field-induced XY antiferromagnetic phase. The ability to tune the structure of polymeric materials is much enhanced compared to the ability in similar materials based on oxide chemistry and will allow further exploration of the magnetic properties of these systems using applied pressure and chemical methods. This work also demonstrates the potential for creating still more exotic magnetic ground states from coordination polymers such as Cu-pyz systems. Indeed, through chemically engineering frustration into such a system, a spin-liquid ground state might be achieved.

[*]tom.lancaster@durham.ac.uk
[†]Present address: Division of Materials Research, National Science Foundation, 4201 Wilson Boulevard, Arlington, VA 22230, USA.
[‡]jmanson@ewu.edu

[1] S. R. Batten, S. M. Neville, and D. R. Turner, *Coordination Polymers: Design, Analysis and Application* (RSC, Cambridge, 2009).

[2] P. A. Goddard *et al.*, Phys. Rev. Lett. **108**, 077208 (2012).

[3] T. Giamarchi, *Quantum Physics in One Dimension* (Oxford University Press, Oxford, 2004).

[4] T. Giamarchi, C. Rüegg, and O. Tchernyshyov, Nat. Phys. **4**, 198 (2008).

[5] A. Zheludev and T. Roscilde, C. R. Phys. **14**, 740 (2013).

[6] See Supplemental Material at http://link.aps.org/supplemental/10.1103/PhysRevLett.112.207201 for a description of the synthesis, structure determination, experimental details and further analysis of the μ^+SR and EPR data.

[7] D. C. Johnston, R. K. Kremer, M. Troyer, X. Wang, A. Klümper, S. L. Bud'ko, A. F. Panchula, and P. C. Canfield, Phys. Rev. B **61**, 9558 (2000).

[8] P. A. Goddard *et al.*, New J. Phys. **10**, 083025 (2008).

[9] P. Sengupta, A. W. Sandvik, and R. R. P. Singh, Phys. Rev. B **68**, 094423 (2003).

[10] T. Lancaster, S. J. Blundell, M. L. Brooks, P. J. Baker, F. L. Pratt, J. L. Manson, C. P. Landee, and C. Baines, Phys. Rev. B **73**, 020410(R) (2006).

[11] C. Yasuda, S. Todo, K. Hukushima, F. Alet, M. Keller, M. Troyer, and H. Takayama, Phys. Rev. Lett. **94**, 217201 (2005).

[12] A. Keren, L. P. Le, G. M. Luke, B. J. Sternlieb, W. D. Wu, Y. J. Uemura, S. Tajima, and S. Uchida, Phys. Rev. B **48**, 12926 (1993).

[13] F. L. Pratt, S. J. Blundell, T. Lancaster, C. Baines, and S. Takagi, Phys. Rev. Lett. **96**, 247203 (2006).

[14] B. Bleaney and K. A. Bowers, Proc. R. Soc. A **214**, 451 (1952).

[15] S. Ghannadzadeh, M. Coak, I. Franke, P. A. Goddard, J. Singleton, and J. L. Manson, Rev. Sci. Instrum. **82**, 113902 (2011)

[16] A. J. Steele, T. Lancaster, S. J. Blundell, P. J. Baker, F. L. Pratt, C. Baines, M. M. Conner, H. I. Southerland, J. L. Manson, and J. A. Schlueter, Phys. Rev. B **84**, 064412 (2011).

[17] B. S. Conner, H. D. Zhou, Y. J. Jo, L. Balicas, C. R. Wiebe, J. P. Carlo, Y. J. Uemura, A. A. Aczel, T. J. Williams, and G. M. Luke, Phys. Rev. B **81**, 132401 (2010).

[18] M. Tachiki and T. Yamada, J. Phys. Soc. Jpn. **28**, 1413 (1970).

[19] T. Giamarchi and A. M. Tsvelik, Phys. Rev. B **59**, 11398 (1999).

[20] K. Yosida, *Theory of Magnetism* (Springer-Verlag, Berlin, 1996).